

AMIR BIJAN YASREBI*¹, ANDREW WETHERELT*, PATRICK J. FOSTER*,
PEYMAN AFZAL***, JOHN COGGAN*, DARIUSH KAVEH AHANGARAN*

APPLICATION OF RQD-NUMBER AND RQD-VOLUME MULTIFRACTAL MODELLING TO DELINEATE ROCK MASS CHARACTERISATION IN KAHANG Cu-Mo PORPHYRY DEPOSIT, CENTRAL IRAN

ZASTOSOWANIE METOD MODELOWANIA NUMERYCZNEGO ORAZ MODELOWANIA FRAKTALNEGO DO ANALIZY JAKOŚCI SKAŁ W CELU OKREŚLENIA CHARAKTERYSTYKI GÓROTWORU W OBSZARZE ZŁOŻA Cu-Mo W KAHANG, ŚRODKOWY IRAN

Identification of rock mass properties in terms of Rock Quality Designation (RQD) plays a significant role in mine planning and design. This study aims to separate the rock mass characterisation based on RQD data analysed from 48 boreholes in Kahang Cu-Mo porphyry deposit situated in the central Iran utilising RQD-Volume (RQD-V) and RQD-Number (RQD-N) fractal models. The log-log plots for RQD-V and RQD-N models show four rock mass populations defined by RQD thresholds of 3.55, 25.12 and 89.12% and 10.47, 41.68 and 83.17% respectively which represent very poor, poor, good and excellent rocks based on Deere and Miller rock classification. The RQD-V and RQD-N models indicate that the excellent rocks are situated in the NW and central parts of this deposit however, the good rocks are located in the most parts of the deposit. The results of validation of the fractal models with the RQD block model show that the RQD-N fractal model of excellent rock quality is better than the RQD-V fractal model of the same rock quality. Correlation between results of the fractal and the geological models illustrates that the excellent rocks are associated with porphyric quartz diorite (PQD) units. The results reveal that there is a multifractal nature in rock characterisation with respect to RQD for the Kahang deposit. The proposed fractal model can be intended for the better understanding of the rock quality for purpose of determination of the final pit slope.

Keywords: RQD, RQD-V & RQD-N fractal models, Kahang Cu-Mo porphyry, porphyric quartz diorite, Central Iran

Identyfikacja właściwości górotworu odgrywa zasadniczą rolę w planowaniu wydobycia i projektowaniu kopalni. Praca niniejsza ma na celu określenie charakterystyki górotworu w oparciu o dane o jakości skał zebrane na podstawie próbek uzyskanych z 48 odwiertów wykonanych w złożu porfiry Cu-Mo w Kahang, zalegającym w środkowym Iranie przy użyciu modeli fraktalnych RQD-V – Rock Quality De-

* CAMBORNE SCHOOL OF MINES, UNIVERSITY OF EXETER, PENRYN, UK

** DEPARTMENT OF MINING ENGINEERING, SOUTH TEHRAN BRANCH, ISLAMIC AZAD UNIVERSITY, TEHRAN, IRAN

¹ CORRESPONDING AUTHOR: aby203@exeter.ac.uk

termination-Volume [Określenie jakości skał-objętość]) i RQD-N (Rock Quality Determination-Number [Określenie jakości skał-liczba]). Wykresy logarytmiczne wykonane dla modeli RQD-V i RQD-N wykazują istnienie czterech populacji warstw górotworu, określonych na podstawie parametrów progowych: 3.55; 25.12; 89.12% oraz 10.47; 41.68 i 83.17%, odpowiadającym kolejno stopniom jakości: bardzo słaby, słaby, dobry i bardzo dobry, zgodnie z klasyfikacją skał Deere i Millera. Wyniki uzyskane przy zastosowaniu modeli RQD-V i RQD-N wskazują, że najlepsze skały zalegają w północno- zachodniej i centralnej części złoża, z kolei dobrej jakości skały znaleźć można w obrębie całego złoża. Walidacja modeli fraktalnych w oparciu o model blokowy (RQD block model) wskazuje, że model RQD-N dla bardzo dobrej jakości skał jest skuteczniejszy niż model RQD-V dla tej samej jakości skał. Wysoki stopień korelacji pomiędzy wynikami uzyskanymi w oparciu o modele fraktalne i geologiczne pokazuje, że najwyższej jakości skały związane są z obecnością porfirowego diorytu kwarcowego. Badanie wykazuje fraktalną naturę charakterystyki jakości skał w złożu Kahang. Zaproponowany model fraktalny wykorzystać można do lepszego poznania zagadnienia jakości skał w celu obliczenia nachylenia wyrobiska.

Słowa kluczowe: określenie właściwości górotworu, modele fraktalne RQD-V i RQD-N, złożo porfiru Cu-MO w Kahang, porfirowy dioryt kwarcowy, środkowy Iran

1. Introduction

Separation of rock mass characterisation based on RQD is essential in mineral exploration, resource evaluation and mine planning because the cost of mining is relevant to the final pit slope due to the variation of strip ratio (Huströlid & Kuchta, 2006). Host rocks of porphyry deposits consist of sub-volcanic massive ore bodies such as porphyritic quartz diorite, granite, monzonite and quartz monzonite which are lithological units with high hardness (Hitzman et al., 1992; Laznicka, 2005). Variations of lithological units are other useful parameters for identification of rock mass characterisation in the porphyry deposits.

The mathematical models have been hugely intended to explain various phenomena for better understanding and interpretation predominantly in mining-based issues such as lithology, density, rock mass characterisation and RQD analysis (Jinga & Hudson, 2002; Lina & Kub, 2006; Rafiee & Vinches, 2008). A number of models have been used towards purpose of modelling based on statistical, geostatistical and fractal theories (Boadu & Long, 1994; Ehlen, 2000; Ghosh & Daemem, 1993; Hamdi & Mouza, 2005). However, the classical statistics methods for delineation of populations from background such as histogram analysis, box plot, summation of mean and standard deviation coefficients and median are not sufficient because the statistical methods consider only the frequency distribution of information (such as RQD data particularly in this scenario) while have no attention to spatial variability since the information about the spatial correlation is not always available (Galuszka, 2007; Hawkes & Webb, 1962; 1979; Reiman et al., 2005; Stanley & Sinclair, 1989; Tukey, 1977). In addition, these methods are only applicable to cases where data follows a normal distribution (Afzal et al., 2012; Bai et al., 2010; Carranza, 2008; Davis, 2002; Li et al., 2003).

The fractal modelling as an important branch of nonlinear mathematical sciences, which was introduced by Mandelbrot (1983), has been applicable in the geosciences and mining engineering since the 1980s (e.g., Agterberg et al., 1993; Ali et al., 2007; Cheng et al., 1994; Goncalves et al., 2001; Sim et al., 1999; Turcotte, 1986; Shen & Zhao, 2002). As a result, several fractal models have been proposed to rock characterisation, geophysical and geochemical exploration for delineation of different populations (Afzal et al., 2011; Agterberg et al., 1993; Cheng et al., 1994; Daneshvar Saein et al., 2012; Delavar et al., 2012; Sadeghi et al., 2012; Xie, 1993). So therefore, the RQD-V and RQD-N models based on multifractal modelling can be employed to

illustrate the distribution of RQD populations without pre-processing of data. The RQD-V and RQD-N fractal models indicate that there is a relationship between desirable attributes (e.g., RQD values within the deposit) and their cumulative numbers of samples in this studied area. In other words, variations of fractal dimensions in RQD data can clarify applicable criteria to identify rock mass characterisation within a study area.

The aim of this study is to expand the application of fractal geometry in related mining engineering. Following the RQD-Volume (RQD-V) and RQD-Number (RQD-N) fractal models are proposed to recognise various rock mass populations in major rock types according to RQD data in the Kahang Cu-Mo porphyry deposit, central Iran. Then, the obtained results via both proposed fractal models are correlated and validated with porphyric quartz diorite (PQD) units (as the major host rock) and also Deere and Miller rock classification (1966) to address which of the proposed fractal models has the proper results with respect to the amount of voxels (blocks) located and categorised in the mentioned lithology unit and rock classification respectively.

2. Geological setting of the Kahang Cu-Mo porphyry deposit

The Kahang deposit is located about 73 km NE of Isfahan in central Iran. The deposit is situated in the Cenozoic Urumieh-Dokhtar magmatic belt extending from NW to SE Iran depicted in Fig. 1 (Alavi, 1994; Berberian & King, 1981; Dargahi et al., 2010). This deposit is mainly composed of Eocene volcanic-pyroclastic rocks, which were intruded by quartz monzonite, monzogranite-diorite to dioritic intrusions in Oligo-Miocene rocks (Fig. 1). The extrusive rocks, including tuffs, breccias and lavas are dacitic to andesitic composition.

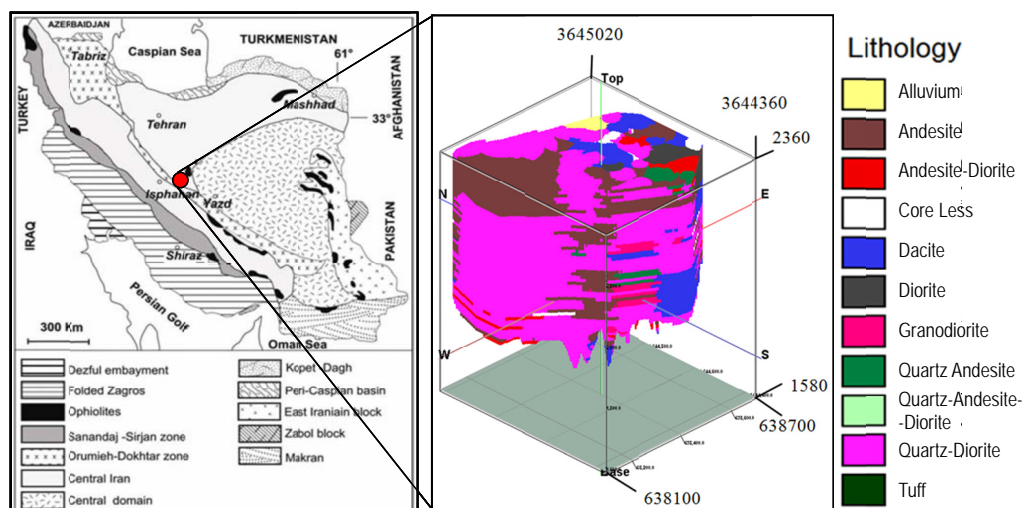


Fig. 1. Lithological 3D model of Kahang porphyry deposit within Urumieh-Dokhtar volcanic belt in structural map of Iran (Alavi, 1994)

The main structural features are two fault systems trending NE-SW and NW-SE. The major alteration zones of potassic, phyllic, argillic and propylitic types were accompanied by the vein to veinlets fillings of quartz, quartz-magnetite and Fe-hydroxides. Mineralisation within intrusives bodies and their surrounding host rocks consists of chalcocite, chalcopyrite, pyrite, malachite, magnetite, limonite jarosite, goethite and chalcantite in quartz stockworks and advanced argillic alteration. The eastern part of the deposit is covered by phyllic and quartz-sericite alteration (Afzal et al., 2010; Rashidnejad Omran et al., 2011).

3. Methodology

A database was generated based on RQD values and the dataset was entered into the Rock-Works15 software package to build up a 3D RQD block models (Fig. 2) utilising Inverse Distance Weighted (IDW) anisotropy as the estimator. The project dimensions are $600 \times 660 \times 780$ m in X, Y and Z direction and each voxel has a dimension of $4 \times 4 \times 10$ m respectively. The next step is to propose the RQD-V and RQD-N fractal models for the identification of different populations in terms of RQD. Subsequently, a mathematical facility of the software called Multiple of Model & Model as a tool to manipulate the voxels in a solid model by the corresponding voxels in another equally-dimensioned solid model file has been intended for combination between the RQD 3D block model interpreted via RQD-V and RQD-N fractal models and the most frequent host rock which is porphyric quartz diorite (Fig. 3) including Cu-Mo ore accumulation as the index of sub-volcanic acidic rocks.

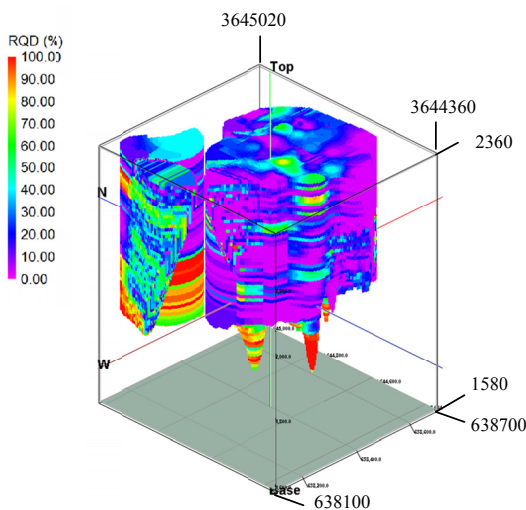


Fig. 2. RQD block model in Kahang porphyry deposit

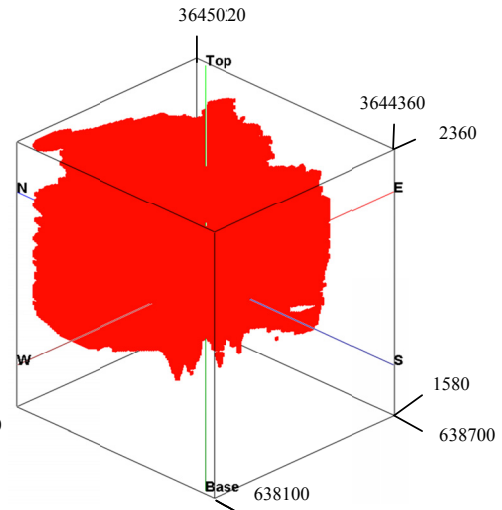


Fig. 3. Porphyric quartz diorite unit within the deposit

4. Fractal Models

4.1. RQD-Number (RQD-N) Fractal Model

The model is expressed by the following equation (Agterberg, 1995; Deng et al., 2010; Mandelbrot, 1983):

$$N(\geq \rho) = F\rho^{-D} \quad (1)$$

where ρ denotes RQD values, $N(\geq \rho)$ denotes cumulative number of samples with RQD values greater than or equal to ρ , F is a constant and D is the scaling exponent or fractal dimension of the distribution of RQD values. According to Mandelbrot (1983) and Deng et al. (2010), log–log plots of $N(\geq \rho)$ versus ρ show straight line segments with different slopes $-D$ corresponding to different RQD intervals.

4.2. RQD-Volume (RQD-V) fractal model

The RQD–V fractal model which is developed based on Concentration-Volume (C-V) fractal model by Afzal et al. (2011) for separation of rock populations based on RQD as an important parameter for the rock mass characterisation, can be expressed as:

$$V(\rho \leq v)\mu\rho^{-a1}; V(\rho \geq v)\mu\rho^{-a2} \quad (2)$$

where $V(\rho \leq v)$ and $V(\rho \geq v)$ denote two volumes with RQD values less than or equal to and greater than or equal to the contour value ρ ; v represents the threshold value of a volume; and $a1$ and $a2$ are characteristic exponents. Threshold values in this model represent boundaries between different rock mass populations of mineral deposits. To calculate $V(\rho \leq v)$ and $V(\rho \geq v)$, which are the volumes enclosed by a contour level ρ in a 3D model, the borehole data of RQD values were interpolated by using geostatistical and IDW estimation.

5. Application of RQD-V and RQD-N fractal modelling

From 42 out of 48 drillcores (Fig. 4) within the deposit, 14976 RQD samples have been collected at 2 m intervals. The distribution of number of samples among 42 drillcores is presented in Table 1. The distribution of RQD data indicates bi-modal nature with RQD mean value of 48.50% (Fig. 5). The derived block model was used as input to the RQD-V model. The Kahang deposit was modelled with 489,927 voxels and each voxel has a dimension of $4 \times 4 \times 10$ m in the X, Y and Z directions which were determined based on the geometrical properties of the deposit and grid drilling dimensions (David, 1970). The terms of “very poor”, “poor”, “fair”, “good” and “excellent” rocks have been used to classify rock mass characterisation based on fractal models and in accordance with the Deere and Miller rock classification.

TABLE 1

Distribution number of RQD samples among drillcores in the Kahang deposit

Drillcore	Kag_03	Kag_04	Kag_05	Kag_06	Kag_07	Kag_08	Kag_09	Kag_10	Kag_11	Kag_12	Kag_13	Kag_14	Kag_15	Kag_17	Kag_18	Kag_19
Samples	547	406	265	382	440	438	401	351	428	504	372	267	239	291	265	395
Drillcore	Kag_20	Kag_27	Kag_28	Kag_30	Kag_33	Kag_36	Kag_38	Kag_41	Kag_42	Kag_43	Kag_46	Kag_47	Kag_48	Kag_49	Kag_50	Kag_51
Samples	329	330	437	377	131	435	301	458	328	254	437	310	434	541	331	341
Drillcore	Kag_52	Kag_54	Kag_55	Kag_57	Kag_59	KH-DDH02		KH-DDH09		KH-DDH10		KH-DDH11		KH-DDH12		
Samples	434	444	365	415	353	128		210		274		279		309		

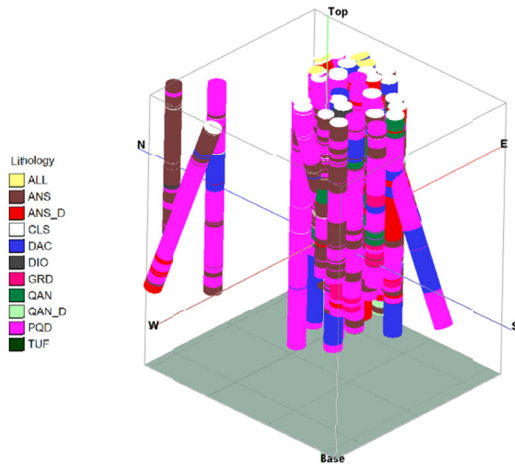


Fig. 4. The locations of drillcores within the Kahang deposit

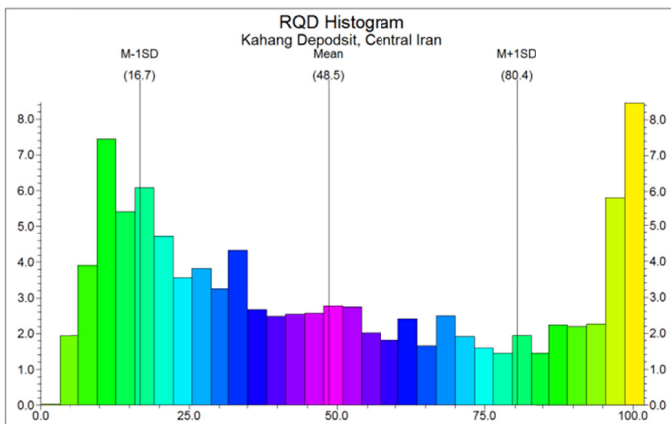


Fig. 5. Histogram of RQD in the Kahang deposit

5.1. RQD-N fractal modelling

The RQD-N method was applied to the RQD data (samples). The selection of breakpoints as threshold values appears to be an objective decision due to the RQD populations which are determined by different segments in the RQD-N log-log plot (Fig. 6). In other words, the intensity of RQD enrichment is depicted by each slope of the line segment in the log-log plot. Accordingly, there are four populations with respect to RQD data. The first RQD threshold is 10.47 and values of <10.47 RQD pertain to very poor rock characterisation. The second RQD threshold is 41.68 and values of $10.47 < \text{RQD} < 41.68$ for RQD pertain to poor rock type whereas the third threshold of 83.17 for the populations of $41.68 < \text{RQD} < 83.17$ represent a combination of fair and good rock mass classification. The values >83.17 for RQD pertain to the excellent rock quality (Table 2).

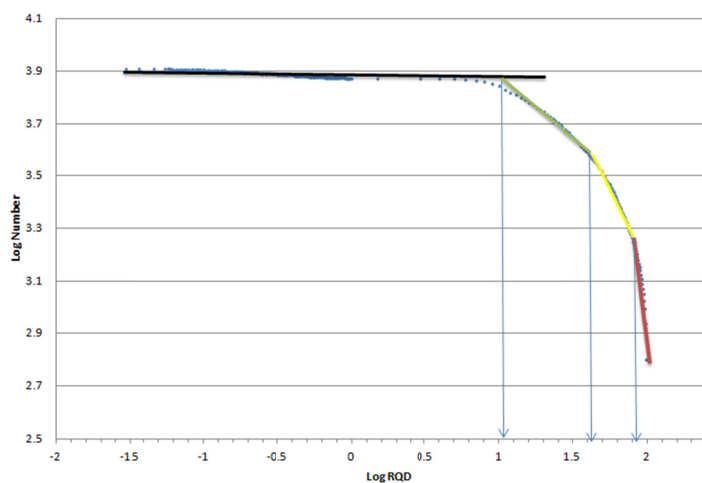


Fig. 6. RQD-N log-log plot in the Kahang deposit

The various zones with different RQD values with respect to RQD-N fractal model were distinguished by a mathematical filter facility of RockWorks software which is called “Boolean data type”. As a result, the studied zones in the RQD 3D model are allocated with binary codes (zero or one) which represent that the zones with the code number of zero are removed and the zones with the code number of one will be remaining in the 3D model. In other words, this tool transforms a real number solid model file to a Boolean (true/false) file. In this process, the RQD values of nodes are set to “1” if their original value falls within a user-specified range and to a “0” if the RQD values do not fall within the range. Then, it runs the Boolean model through available filters or multiplies it to the original model to zero-out areas where the desired criteria are not met.

Based on classification of the 3D model of the RQD data and based on the thresholds obtained from the RQD-N fractal model, very poor and poor zones are situated in the most parts of the deposit. Fair and good rock mass classifications of the studied area are scattered in the most parts of the Kahang deposit especially in the majority of NE. However, the excellent rock type is in the central and NW parts of the deposit (Fig. 7).

TABLE 2

RQD populations (zones) based on three thresholds defined from RQD-N fractal model

Deere and Miller RQD classification	RQD Range obtained by RQD-N log-log plot	The amount of voxels in each RQD range
Very Poor	<10.47	147695
Very poor & Poor	10.47 – 41.68	188663
Fair & Good	41.68 – 83.17	88647
Excellent	>83.17	43098

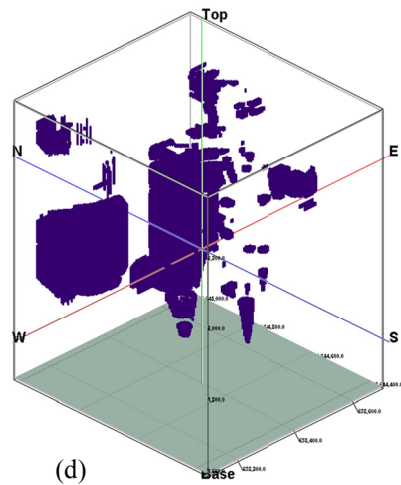
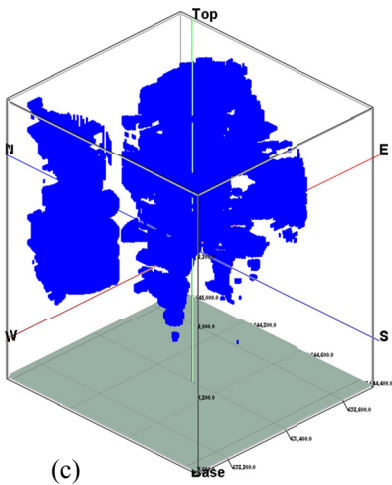
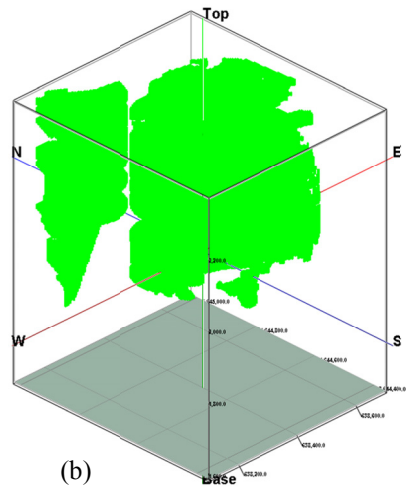
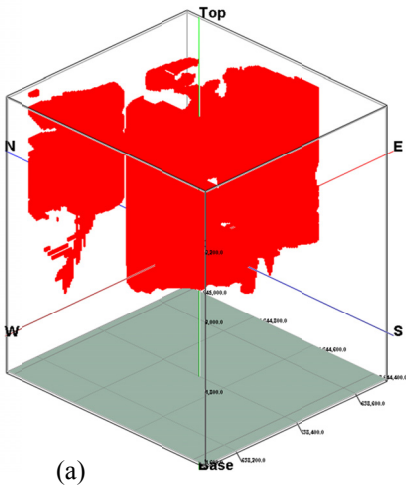


Fig. 7. RQD populations in the Kahang deposit based on thresholds defined from the RQD-N fractal model (a) very poor zones; (b) very poor & poor zones; (c) fair and good zones; (d) excellent zones

5.2. RQD-V fractal modelling

According to the RQD 3D block model, volumes corresponding to various RQD values were calculated to derive a RQD-V fractal model. Threshold values of RQD were recognised in the RQD-V log-log plot (Fig. 8) which reveals a power-law relationship between RQD values and volumes occupied. Depicted arrows in the log-log plot illustrate threshold values as three breakpoints corresponding to 3.55, 25.12 and 89.12 for RQD. Based on the log-log plot, the excellent RQD populations are considered to have >89.12 (Table 3). The range of RQD values between 89.12 and 25.12 indicate a combination of goof, fair and poor rock mass quality. However, very poor rock characterisation is for $RQD < 25.12$ containing of threshold value equal to 3.55 so therefore, there are two very poor RQD populations in this deposit considering RQD-V fractal modelling.

TABLE 3

RQD populations (zones) based on three thresholds defined from RQD-V fractal model

Deere and Miller RQD classification	RQD Range obtained by RQD-V log-log plot	The amount of voxels in each RQD range
Very Poor	<3.55	66015
Very poor	3.55 – 25.12	191307
Poor, Fair & Good	25.12 – 89.12	180461
Excellent	>89.12	30244

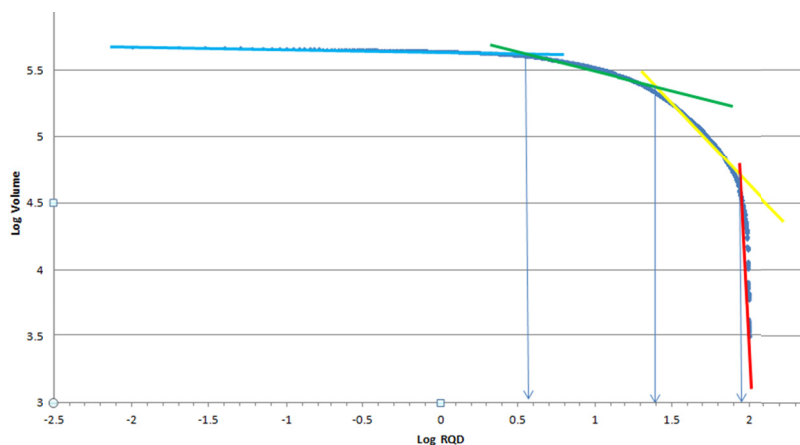


Fig. 8. RQD-V log-log plot in the Kahang deposit

Based on the RQD-V fractal model, very poor zones are situated in most part of the deposit (Fig. 9). However, poor, fair and good zones are along NE-NW trend. Excellent zones in terms of RQD occur in the central and NW parts of the deposit. As a result, for $RQD > 89.12$ the slope of the straight line fit is near to 90° based on the RQD-V log-log plot.

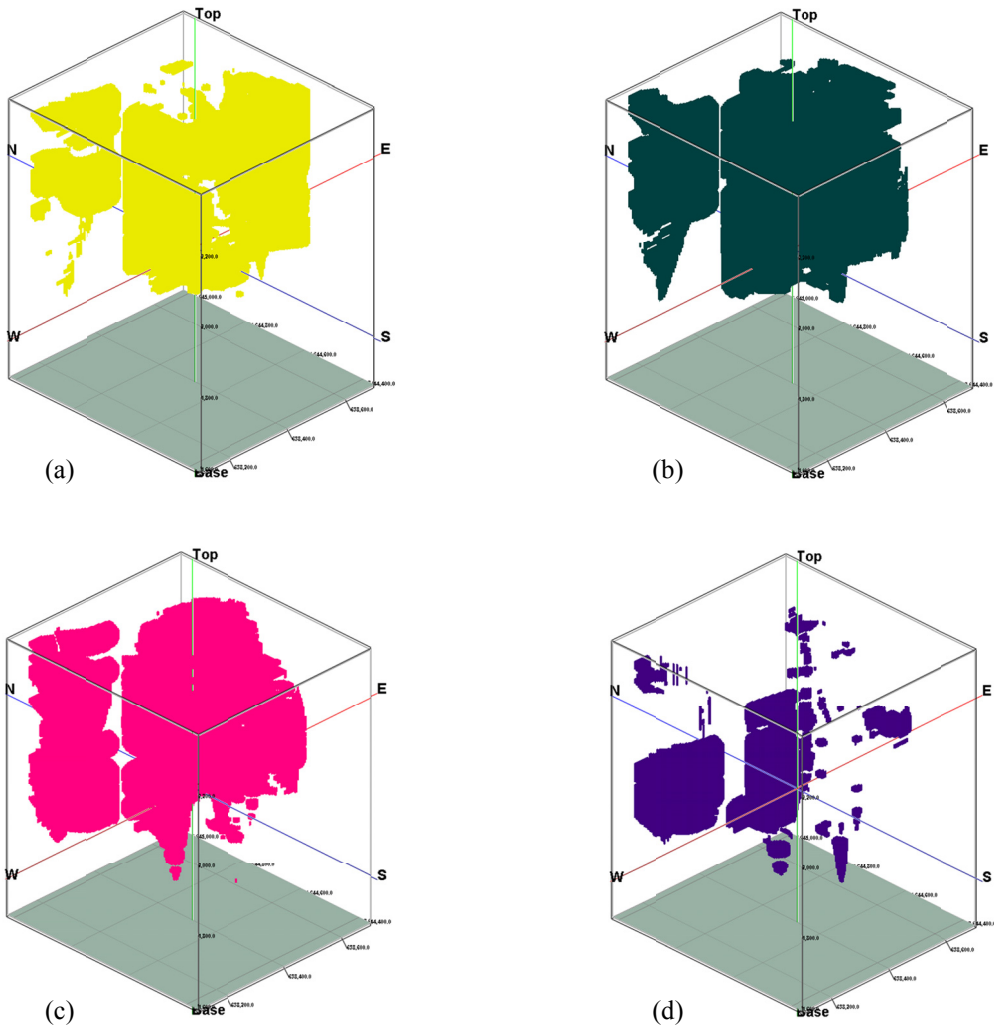


Fig. 9. RQD populations in the Kahang deposit based on thresholds defined from the RQD-V fractal model (a) very poor zones; (b) very poor zones; (c) poor, fair and good zones; (d) excellent zones

6. Correlation of fractal models with excellent RQD values in porphyritic quartz diorite units

Results of the RQD-N and RQD-V models are correlated to the major lithological units of the deposit consisting of porphyritic quartz diorite constructed by using RockWorks™ v. 15 software and drillcore data (Fig. 3). Rocks with excellent RQD defined by means of the RQD-N and RQD-V models are well-correlated with porphyritic quartz diorite defined by the 3D modelling of lithological drillcores data. As a result, there is spatial coincidence between excellent

rock mass characterisation driven via means of the RQD-N and RQD-V models and porphyritic quartz diorite defined by 3D modelling of geological drillcore data in the central and NW parts of the deposit (Fig. 10). Therefore, it can be concluded that the porphyritic quartz diorite units host the excellent values for RQD.

7. Conclusion

In this paper, the RQD-Number (RQD-N-S) and RQD-Volume (RQD-V) fractal models were used to investigate and delineate various RQD populations in the Kahang Cu-Mo porphyry deposit (Central Iran). Both the RQD-N and RQD-V fractal models illustrate four RQD populations in the deposit. The threshold RQD values for excellent rocks are 83.17 and 89.12 based on the fractal models as situated in the central and NW parts of the deposit. Models of good and fair rocks in the central, eastern and NW parts of the deposit contain 41.68–83.17 RQD according to the RQD-N model, and 25.12–89.12 RQD according to the RQD-V model. According to the correlation between results driven by fractal modeling and major lithological unit (porphyritic quartz diorite) in the Kahang deposit, rocks with excellent RQD defined by means of the RQD-N and RQD-V models, especially the RQD-N model, have a strong correlation with porphyritic quartz diorites resulted by the 3D geological model.

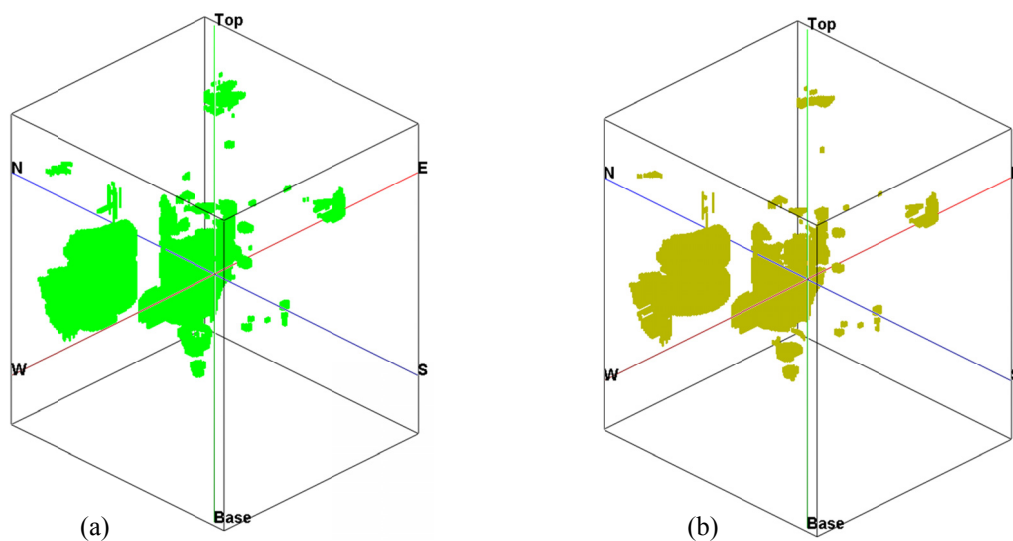


Fig. 10. 3D Model of porphyritic quartz diorite units based on:
(a) RQD-N model for RQD > 83.17; (b) RQD-V model for RQD > 89.12

Acknowledgments

The authors are grateful to the National Iranian Copper Industries Co. (NICICO) for their permission to have access to the Kahang deposit dataset. Additionally, the authors would like to thank Mr. Reza Esfahanipour the head of Exploration and Development Department of the NICICO for his support.

The authors also are hugely thankful to the Institute of Materials, Minerals and Mining (IOM3) for its financial support in order to conduct this research.

References

- Afzal P., Fadakar Alghalandis Y., Khakzad A., Moarefvand P., Rashidnejad Omran N., Asadi Haroni H., 2012. *Application of power-spectrum–volume fractal method for detecting hypogene, supergene enrichment, leached and barren zones in Kahang Cu porphyry deposit, Central Iran*. Journal of Geochemical Exploration 112, 131-138.
- Afzal P., Fadakar Alghalandis Y., Khakzad A., Moarefvand P., Rashidnejad Omran N., 2011. *Delineation of mineralization zones in porphyry Cu deposits by fractal concentration–volume modelling*. Journal of Geochemical Exploration 108, 220-232.
- Afzal P., Khakzad A., Moarefvand P., Rashidnejad Omran N., Esfandiari B., Fadakar Alghalandis Y., 2010. *Geochemical anomaly separation by multifractal modelling in Kahang (Gor Gor) porphyry system, Central Iran*. Journal of Geochemical Exploration 104, 34-46.
- Agterberg F.P., Cheng Q., Wright D.F., 1993. *Fractal modeling of mineral deposits*. In: Elbrond, J., Tang, X. (Eds.), 24th APCOM symposium proceeding, Montreal, Canada, pp. 43-53.
- Agterberg F.P., 1995. *Multifractal modeling of the sizes and grades of giant and supergiant deposits*. International Geology Review 37, 1-8.
- Alavi M., 1994. *Tectonic of Zagros orogenic belt of Iran: new data and interpretations*. Tectonophysics 229, 211-238.
- Ali Kh., Cheng Q., Zhijun C., 2007. *Multifractal power spectrum and singularity analysis for modelling stream sediment geochemical distribution patterns to identify anomalies related to gold mineralization in Yunnan Province, South China*. Geochemistry: Exploration, Environment, Analysis 7 (4), 293-301.
- Bai J., Porwal A., Hart C., Ford A., Yu L., 2010. *Mapping geochemical singularity using multifractal analysis: application to anomaly definition on stream sediments data from Funin Sheet, Yunnan, China*. Journal of Geochemical Exploration 104, 1-11.
- Berberian M., King G.C., 1981. *Towards a paleogeography and tectonic evolution of Iran*. Canadian Journal of Earth Sciences 18, 210-265.
- Boadu F.K., Long L.T., 1994. *The fractal character of fracture spacing and RQD*. International Journal of Rock Mechanics and Mining Sciences & Geomechanics Abstracts 31, 127-134.
- Carranza E.J.M., 2008. *Geochemical anomaly and mineral prospectivity mapping in GIS*. Handbook of Exploration and Environmental Geochemistry, Vol. 11. Elsevier, Amsterdam. 351 pp.
- Cheng Q., Agterberg F.P., Ballantyne S.B., 1994. *The separation of geochemical anomalies from background by fractal methods*. Journal of Geochemical Exploration 51, 109-130.
- Daneshvar Saein L., Rasa I., Rashidnejad Omran N., Moarefvand P., Afzal P., 2012. *Application of concentration-volume fractal method in induced polarization and resistivity data interpretation for Cu-Mo porphyry deposits exploration, case study: Nowchun Cu-Mo deposit, SE Iran*. Nonlinear Processes in Geophysics 19, 431-438.
- Dargahi S., Arvin M., Pan Y., Babaei A., 2010. *Petrogenesis of post-collisional A-type granitoids from the Urumieh–Dokhtar magmatic assemblage, Southwestern Kerman, Iran: Constraints on the Arabian–Eurasian continental collision*. Lithos 115, 190-204.
- David M., 1977. *Geostatistical Ore Reserve Estimation*. Amsterdam: Elsevier, 283 p.
- Davis J.C., 2002. *Statistics and data analysis in Geology*. John Wiley and Sons Inc., New York. 638pp.
- Deere D.U., Miller R.P., 1966. *Engineering classification and index properties for intact rock*. Air Force Weapons Laboratory Technical Report AFWL-TR-65-116, 277 p.

- Deng J., Wang Q., Yang L., Wang Y., Gong Q., Liu H., 2010. *Delineation and explanation of geochemical anomalies using fractal models in the Heqing area, Yunnan Province, China*. Journal of Geochemical Exploration 105, 95-105.
- Delavar S.T., Afzal P., Borg G., Rasa I., Lotfi M., Rashidnejad Omran N., 2012. *Delineation of mineralization zones using concentration-volume fractal method in Pb-Zn Carbonate hosted deposits*. Journal of Geochemical Exploration, Journal of Geochemical Exploration 118, 98-11.
- Ehlen J., 2000. *Fractal analysis of joint patterns in granite*. International Journal of Rock Mechanics and Mining Sciences 37, 909-922.
- Gałuszka A., 2007. *A review of geochemical background concepts and an example using data from Poland*. Environmental Geology 52 (5), 861-870.
- Ghosh A., J.K. Daemen J., 1993. *Fractal characteristics of rock discontinuities*. Engineering Geology 34, 1-9.
- Goncalves M.A., Mateus A., Oliveira V., 2001. *Geochemical anomaly separation by multifractal modeling*. Journal of Geochemical Exploration 72, 91-114.
- Hamidi E., Mouza J.D., 2005. *A methodology for rock mass characterisation and classification to improve blast results*. International Journal of Rock Mechanics and Mining Sciences 42, 177-194.
- Hawkes H.E., Webb J.S., 1962. *Geochemistry in Mineral Exploration*. Harper and Row, New York, NY.
- Hawkes H.E., Webb J.S., 1979. *Geochemistry in mineral exploration, 2nd edn*. Academic Press, New York. 657pp.
- Hitzman M.W., Oreskes N., Einaudi M.T., 1992. *Geological characteristics and tectonic setting of Proterozoic iron oxide (Cu-U-Au-REE) deposits*. Precambrian Research 58, 241-287.
- Hustrulid W., Kuchta M., 2006. *Open Pit Mine Planning and Design (2th Edition)*. 972 p.
- Jinga L., Hudson J.A., 2022. *Numerical methods in rock mechanics*. International Journal of Rock Mechanics and Mining Sciences 39, 409-427.
- Laznicka P., 2005. *Giant Metallic Deposits Future Sources of Industrial Metals*. Springer-Verlag. 732 pp.
- Li C., Ma T., Shi J., 2003. *Application of a fractal method relating concentrations and distances for separation of geochemical anomalies from background*. Journal of Geochemical Exploration 77, 167-175.
- Lina J.S., Kub C.Y., 2006. *Two-scale modeling of jointed rock masses*. International Journal of Rock Mechanics and Mining Sciences 43, 426-436.
- Mandelbrot B.B., 1983. *The Fractal Geometry of Nature*. W.H. Freeman, San Francisco, CA. Updated and Augmented Edition.
- Rafiee A., Vinches M., 2008. *Application of geostatistical characteristics of rock mass fracture systems in 3D model generation*. International Journal of Rock Mechanics and Mining Sciences 45, 644-652.
- Rashidnejad Omran N., Afzal P., Harati H., Moarefvand P., Asadi Haroni H., Daneshvar Saein L., 2011. *Application of power-law frequency fractal model in determination of vertical geochemical distribution of Cu in kahang porphyry deposit, Central Iran*. Journal of Mining and Metallurgy, 47 A (1), 1-8.
- Reimann C., Filzmoser P., Garrett R.G., 2005. *Background and threshold: critical comparison of methods of determination*. Sci. Total Environ. 346, 1-16.
- Sadeghi B., Moarefvand P., Afzal P., Yasrebi A.B., Daneshvar Saein L., 2012. *Application of fractal models to outline mineralized zones in the Zaghia iron ore deposit, Central Iran*. Journal of Geochemical Exploration 122, 9-19.
- Stanley C.R., Sinclair A.J., 1989. *Comparison of probability plots and gap statistics in the selection of threshold for exploration geochemistry data*. Journal of Geochemical Exploration 32, 355-357.
- Shen W., Zhao P., 2002. *Theoretical study of statistical fractal model with applications to mineral resource prediction*. Computers & Geosciences 28, 369-376.
- Sim B.L., Agterberg F.P., Beaudry C., 1999. *Determining the cut off between background and relative base metal contamination levels using multifractal methods*. Computers and Geosciences 25, 1023-1041.
- Tukey J.W., 1997. *Exploratory Data Analysis*. Addison-Wesley Publishing Company, Massachusetts, Reading.
- Turcotte D.L., 1986. *A fractal approach to the relationship between ore grade and tonnage*. Economic Geology 18, 1525-1532.
- Xie H., 1993. *Fractals in Rock Mechanics*. Taylor & Francis, 453 p.

Received: 30 November 2012